

A New Finite Element Method for Radiation Transport on Spherical Geodesic Grids

Maitraya K. Bhattacharyya^{1,2}

(with David Radice)

¹Institute for Gravitation and the Cosmos, The Pennsylvania State University

²Department of Physics, The Pennsylvania State University

INT-23-2



PennState

Goals

- Multimessenger astrophysics → binary neutron star mergers
 - Replace current moment-based treatment of neutrino transport in our new NR code!
-
- Limited by numerical resolution due to computational cost → solutions have to look *decent* at low resolutions
 - Robust positivity preservation
 - Ready for next-gen hardware → AthenaK is *performance portable* (GPUs!)

The Boltzmann equation

Distribution function for neutrinos $F(x^\mu, p^\mu)/F(t, x^i, \epsilon, \Omega)$ governed by [Cardall+ 2013]

$$p^{\hat{\mu}} \frac{\partial F}{\partial x^{\hat{\mu}}} - \Gamma^{\hat{i}}_{\hat{\nu}\hat{\mu}} p^{\hat{\nu}} p^{\hat{\mu}} \frac{\partial F}{\partial p^{\hat{i}}} = \mathbb{C}[F],$$

mom. in co-moving frame

$$p^{\hat{\mu}} = (\epsilon, \epsilon \cos \phi \sin \theta, \epsilon \sin \phi \sin \theta, \epsilon \cos \theta)$$

The radiation-matter interaction term [Radice+ 2013]:

$$\mathbb{C}[F] = \frac{c^2 \eta}{h^3 \nu^2} - h\nu(\kappa_a + \kappa_s)F + \frac{h\nu\kappa_s}{4\pi} \int \left(\frac{\nu'}{\nu}\right)^2 K(\vec{p}' \rightarrow \vec{p}) F(\vec{p}') d\nu' d\Omega$$

- special relativity
- single energy
- elastic isotropic scattering
- stationary medium
- $h = c = 1$

$$\frac{\partial F}{\partial t} + p^j \frac{\partial F}{\partial x^j} = \underbrace{\eta}_{\text{emissivity}} + \underbrace{\kappa_a F}_{\text{absorption}} + \underbrace{\kappa_s \left(\frac{E}{4\pi} - F\right)}_{\text{scattering}}, \quad \underbrace{E(t, x^i)}_{\text{energy density}} = \int_{\mathbb{S}_2} F d\Omega.$$

Modeling neutrino transport

Approximate approaches

- Replace BE with more manageable equation
- Phenomenological models: neutrino leakage schemes [van Riper+ 1981, Ruffert+ 1996]
- Moment based methods: Rewrite BE as a sum of moments of F truncated at some finite order → close system [Arnett 1977+, Foucart+ 2015, Radice+ 2022].
- M1: evolves E and first moment i.e. flux,

$$E = \int F d\Omega, \quad F^i = \int F p^i d\Omega, \quad P^{ij} = f(E, F^i).$$

- Inexpensive, but not BE continuum limit.
- Accuracy depends on choice of closure [Garett & Hauck 2013], so choose wisely [Schotthöfer+ 2022]

Boltzmann solvers

- 1D [Mezzacapa+ 1993, Sumiyoshi+ 2005], 2D [Livne+ 2004], 3D [Sumiyoshi+ 212, 2015]
- Monte Carlo methods [Fleck+ 1971] → stochastic. Explicit schemes expensive in diffusive regime [Cleveland+ 2014], implicit diffusion schemes problematic in GR
- Discrete ordinates (S_N) [Mihalas+ 1984] → Discretize F along N angular bins. “ray effects” seen in regions of low scattering and must be handled with efficient filtering strategies [Hauck+ 2019] See [White+ 2023] for finite volume implementation in AthenaK
- Filtered spherical harmonics (FP_N) [McClarren+ 2010] → rotational invariance but oscillations → filtering is needed, limiting [Laiu+ 2019]
- Finite element method for angle → wavelet based refinement schemes [Kópházi+ 2015], multi P_N schemes [Ghazaie+ 2019]

Discretization in angle

Consider N basis functions for angle: $F := F^a \Psi_A$, multiply by Ψ^B , integrate over surface of unit sphere:

$$\Psi_B \times \left(\begin{array}{c} \sum_0^{N-1} F^A(t, x^j) \Psi_A(\Omega) \\ \frac{\partial}{\partial t} \quad \boxed{F} \\ + p^j \frac{\partial F}{\partial x^j} \end{array} \right) = \Psi_B \times \left(\eta + \kappa_a F + \kappa_s \left(\frac{E}{4\pi} - F \right) \right),$$

to obtain the mass, stiffness and source matrices:

$$\int_{\mathbb{S}_2} \Psi^B \Psi_A d\Omega \quad \int_{\mathbb{S}_2} p^j \Psi^B \Psi_A d\Omega \quad \int_{\mathbb{S}_2} \eta \Psi^B d\Omega \quad \frac{1}{4\pi} \int_{\mathbb{S}_2} \Psi_B d\Omega' \int_{\mathbb{S}_2} \kappa_s \Psi^A d\Omega - \delta_B^A$$

$$\boxed{M_A^B} \quad \frac{\partial F^A}{\partial t} + \quad \boxed{S_A^B} \quad \frac{\partial F^A}{\partial x^j} = \quad \boxed{e^B} \quad + \quad \boxed{P_A^B} \quad F^A$$

- M_A^B, S_A^B can be pre-computed. So can the sources under certain cases.
- Choice of Ψ_A determines the scheme. For FP_N , choose real spherical harmonics $\Psi_A = Y_{lm}(\theta, \phi)$ [Radice+ 2013]. Then $M_A^B = \delta_A^B$.

Geodesic grids

- All points on the grid represented in cartesian coordinates to avoid singularities.
- All triangular elements of the grid have almost equal area.
- Base grid: A regular icosahedron on a unit sphere [Giraldo 1997]:

$$\vec{x} = \left\{ \frac{1}{\sqrt{1+\varphi^2}}(0, \pm 1, \pm \varphi), \frac{1}{\sqrt{1+\varphi^2}}(\pm 1, \pm \varphi, 0), \frac{1}{\sqrt{1+\varphi^2}}(\pm \varphi, 0, \pm 1) \right\}$$

- Refinement: For an edge (\vec{x}_A, \vec{x}_B) of a Δ , find \vec{x}_C projected on unit sphere

$$\vec{x}_C = \frac{(\vec{x}_A + \vec{x}_B)}{2}, \quad \vec{x}_C = \frac{\vec{x}_C}{|\vec{x}_C|}$$

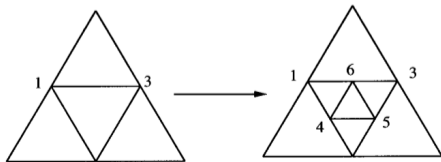
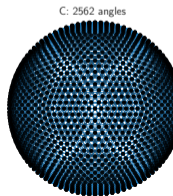
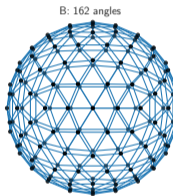
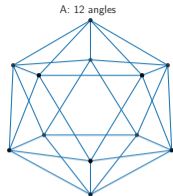


Figure: From Giraldo: Refining by 1 level



Finite element basis functions

For each *triangular element*, use barycentric coordinates to represent basis functions:

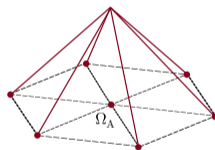
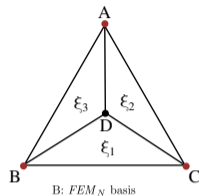
$$\xi_1 = \frac{\Delta_p BCD}{\Delta_p ABC}, \quad \xi_2 = \frac{\Delta_p ACD}{\Delta_p ABC}, \quad \xi_3 = \frac{\Delta_p ABD}{\Delta_p ABC}, \quad \xi_1 + \xi_2 + \xi_3 = 1$$

FEM_N

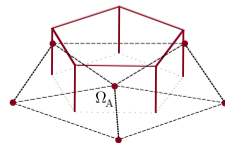
- *coupling between neighboring angles* → “overlapping tent”
- $\Psi_A(\xi_1, \xi_2, \xi_3) = 2\xi_1 + \xi_2 + \xi_3 - 1$

S_N

- “non-overlapping honeycomb”
- $\Psi_A(\xi_1, \xi_2, \xi_3) = \begin{cases} 1, & \xi_1 \geq \xi_2 \text{ and } \xi_1 > \xi_3, \\ 0, & \text{otherwise.} \end{cases}$



C: S_N basis



Discretization in space

- Asymptotic preserving DG scheme \rightarrow correct rates in diffusion dominated regime.
- Divide numerical domain into elements $[x_{i1/2}, x_{i+3/2}]$ comprising two cells with cell centers x_i and x_{i+1}

$$\psi_{i-1/2}(x) = 1 - \frac{x - x_{i-1/2}}{x_{i+3/2} - x_{i-1/2}}, \quad \psi_{i+3/2}(x) = \frac{x - x_{i-1/2}}{x_{i+3/2} - x_{i-1/2}}.$$

- Numerical scheme becomes

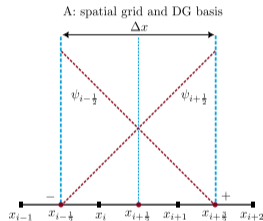
$$\frac{dF_i^A}{dt} = \frac{1}{\Delta x} \mathbb{F}_i^A, \quad \mathbb{F}_i^A \equiv \frac{3}{2} \mathcal{F}^- - \bar{\mathcal{F}} - \frac{1}{2} \mathcal{F}^+, \quad \mathbb{F}_{i+1}^A \equiv \frac{1}{2} \mathcal{F}^- + \bar{\mathcal{F}} - \frac{3}{2} \mathcal{F}^+,$$

with corrections for zero speed modes

$$\mathcal{F}^- = \frac{1}{2} \left[\tilde{\mathcal{S}}^{xA}{}_B \left(F_L^B + F_R^B \right) - \hat{\mathcal{S}}^{xA}{}_B \left(F_R^B - F_L^B \right) \right], \quad \hat{\mathcal{S}}^{xA}{}_B = \mathcal{R}^{xA}{}_C \max(v, |\Lambda^{xC}{}_D|) \mathcal{L}^{xD}{}_B,$$

- Use minmod or double minmod for limiting.

$$\frac{\partial F^A}{\partial t} + \tilde{\mathcal{S}}^{xA}{}_B \frac{\partial F^B}{\partial x} = \mathcal{S}^A[F]$$



Positivity preservation & time integration

FP_N : filtering

- For [Radice+ 2013]

$$F^{\text{new}} = \sum_A \sigma \left(\frac{l}{l_{\text{max}} + 1} \right)^s F^A Y_A,$$

- with filter strength

$$s = -\frac{\Delta t \sigma_{\text{eff}}}{\log \sigma(l/(l+1))}, \quad \sigma(x) = \frac{\sin x}{x}.$$

FEM_N: clipping limiter

- Truncates negative values of F_i^A to zero, readjusts other F_i^A by rescaling by θ :

$$\theta = \frac{\sum_{A,B} M_{AB} F_i^A}{\sum_{A,B} M_{AB} \tilde{F}_i^A}, \quad \tilde{F}_i^A = \max(F_i^A, 0).$$

The values of F_i^A after limiting becomes

$$F_i^{A(\text{new})} = \begin{cases} \theta F_i^A, & \text{if } F_i^A > 0, \\ 0, & \text{if } F_i^A \leq 0. \end{cases}$$

- Conserves E point-wise.

Second-order RK method or a semi-implicit time integrator for the optically thick regime [McClarren+ 2008]

$$F_{k+1/2}^A = F_k^A - \frac{\Delta t}{2} \left(\tilde{S}_{BA}^j \frac{\partial F^A}{\partial x^j} \Big|_k + e_k^A + P_B^A F_{k+1/2}^B \right), \quad F_{k+1}^A = F_k^A - \Delta t \left(\tilde{S}_{BA}^j \frac{\partial F^A}{\partial x^j} \Big|_{k+1/2} + e_{k+1/2}^A + P_B^A F_{k+1}^B \right).$$

Tests: Line source [Ganapol 1999]

- Test angular discretization with radiation pulse

$$F(0, x, y, \Omega) = \frac{1}{4\pi} \delta(x, y).$$

- Analytical solution:

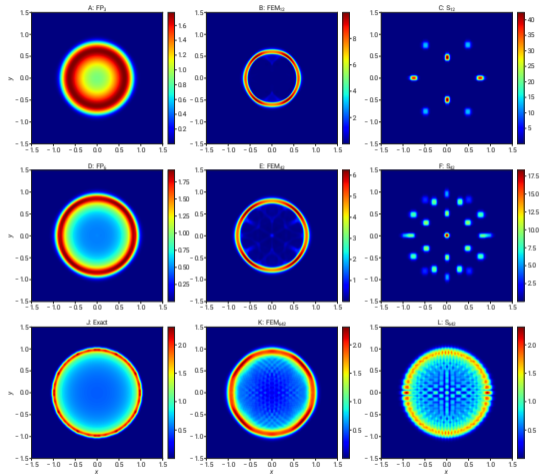
$$\tilde{E}(t, x, y) = \frac{1}{2\pi} \frac{H(t-r)}{t\sqrt{t^2-r^2}}.$$

- Choose ID with $\omega = 0.03$ [Garrett+ 2013]:

$$F(0) = \max\left(\frac{1}{8\pi\omega^2} e^{-(x^2+y^2)/(2\omega^2)}, 10^{-4}\right)$$

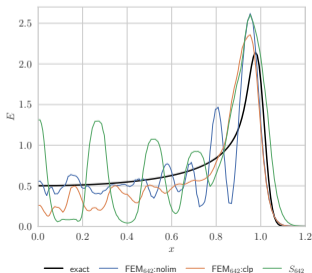
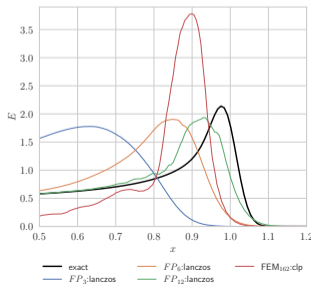
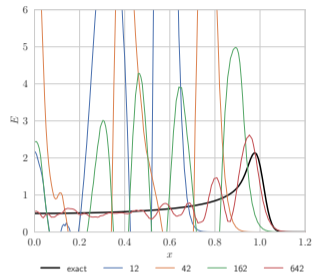
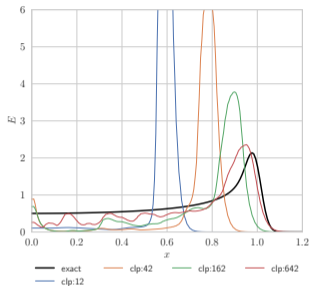
- Solution:

$$E(t, x, y) = \int_{\mathbb{R}^2} E(0, x, y) \tilde{E}(t, x-x', y-y') dx' dy'.$$



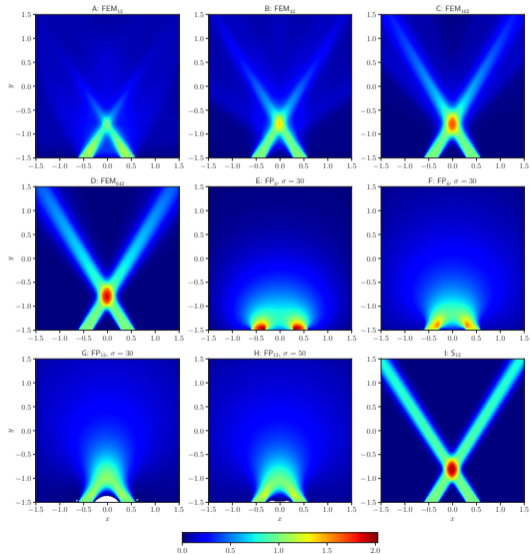
Tests: Line source contd ...

- Top left: Limited FEM_N solutions with angle
- Top right: Non-limited FEM_N solutions with angle
- FP_N and highest resolution FEM_N
- FEM_N and S_N comparison



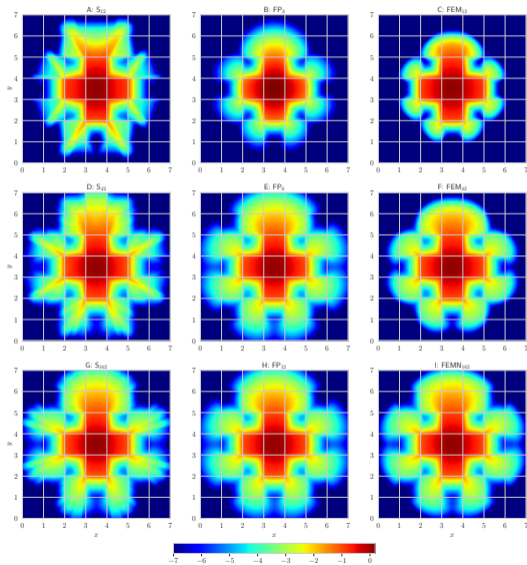
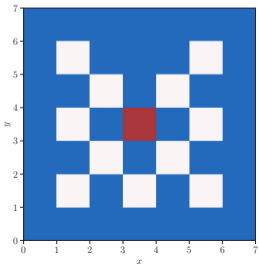
Tests: Beam sources [Stone+ 1992]

- Two narrow beams of radiation propagating in vacuum, evolved till steady state.
- Directed at angles $\phi_1 \approx 58.28^\circ$ and $\phi_2 \approx 121.72^\circ$
- S_N performs the best!
- FEM_N has non-negative solutions which improve with resolution.
- FP_N fails even with filtering.



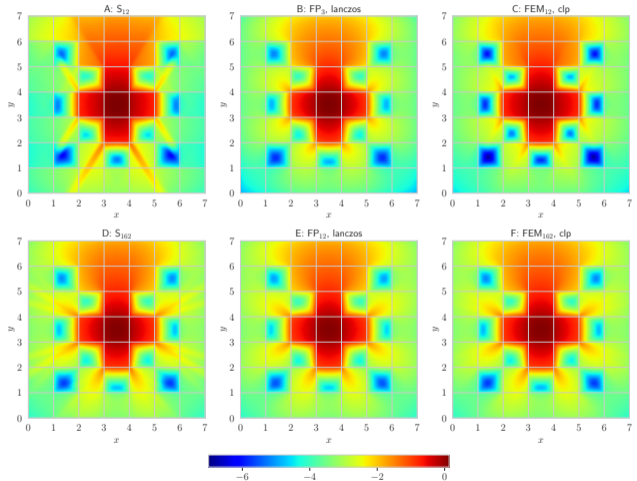
Tests: Lattice [Brunner 2002]

- Test the efficiency of numerical schemes in complex geometries.
- Central emitting square $\eta = 1/4\pi$.
- 11 white absorbing regions $\kappa_a = 1$.
- Blue and red regions are also scattering $\kappa_s = 10$.
- Evolve till $t \approx 3.2$



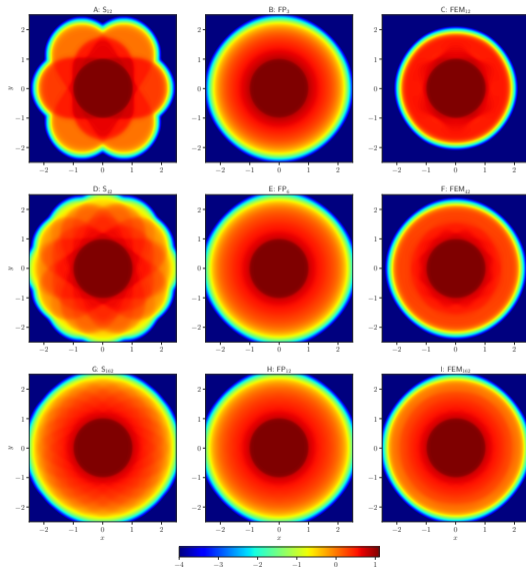
Tests: Lattice contd ...

- Evolved till steady state
- FP_N and FEM_N give comparable results
- Ray-like artifacts demonstrated by S_N solutions



Tests: Cylinder source

- Infinite cylindrical source of radiation of unit radius
- At low angular resolutions, propagation speeds of solutions in the FEM_N and S_N case are slower than the speed of light.
- S_N solutions shown “ray artifacts” and are of worse quality than the solutions produced by the other two methods.



Tests: Cylinder source contd ...

- Steady state exact solution:

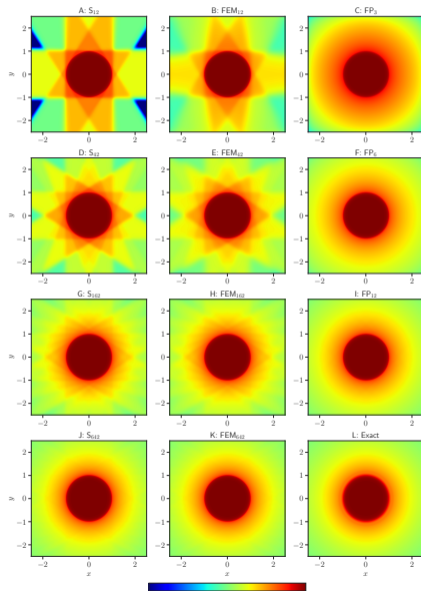
$$F(t, r, \phi, \theta) = \frac{B}{\kappa_a} (1 - e^{-\kappa_a s})$$

where

$$s(r, \phi, \theta) = \lambda_1(r, \phi, \theta) - \lambda_2(r, \phi, \theta)$$

$$\lambda_1 = \max \left(\frac{r \cos \phi - \sqrt{R - r^2 \sin^2 \phi}}{\sin \theta}, 0 \right)$$

$$\lambda_2 = \max \left(\frac{r \cos \phi + \sqrt{R - r^2 \sin^2 \phi}}{\sin \theta}, 0 \right)$$



Conclusions

- Limiting for FEM_N more robust than FP_N for positivity preservation.
- S_N performs worse than FEM_N or FP_N except the line test.
- FP_N solutions sometimes retain small negative values in F . Filtering eliminates it sometimes but at the cost of solution quality.
- A multi-energy GR variant being implemented in AthenaK.

See

Bhattacharyya & Radice, *J. Comput. Phys* (2023), 112365,
doi:10.1016/j.jcp.2023.112365.
(2212.01409)